VISUALISATION OF ACOUSTIC STREAMING USING PIV IN NEWTONIAN AND NON-NEWTONIAN LIQUIDS

MADURANGA AMARATUNGA & RUNE W.TIME
Department of Petroleum Engineering, University of Stavanger, Norway.

ABSTRACT

The effect of fluid rheology on acoustic streaming was studied experimentally using a low frequency (600Hz–15kHz) underwater acoustic transducer. The fluid rheology was compared with deionized water and non-Newtonian fluid polyanionic cellulose (PAC). Streaming effect generated by the transducer in a static liquid medium was visualized by particle image velocimetry (PIV) method. The motion of fluid was optically visualized using light scattering 'seeding' particles. Velocity profiles induced by the acoustic streaming have different shapes and range of magnitudes. First, the acoustic streaming in deionized water was visualized for different frequencies and pressure amplitudes (voltages). A maximum of 1 g/L PAC was then introduced in smaller steps for some selected frequency and voltage settings. The streaming disappeared completely when the total concentration of the fluid medium reached 0.19 g/L PAC. The measured streaming velocities are found to be in the range of 2.1 to 9.9 cm/s for water and it is proportional to the applied voltage and the operating frequency of the transducer. When introducing PAC, the streaming velocity within water gradually decreased until zero due to the attenuation of acoustic waves by viscous effects. This confirms that the streaming velocity is approximately inversely proportional to the bulk viscosity of the medium. The velocity vectors and the streaming velocity maps illustrate the induced non-linearities of the fluid medium due to the acoustic propagation. The results are part of a comprehensive study aimed at investigating the influence of acoustic vibration on particle settling in non-Newtonian fluids.
Keywords: Acoustic streaming, flow visualization, particle image velocimetry, rheology.

1 INTRODUCTION

An acoustic wave is pressure oscillation in a medium, propagation with the sound velocity. For small amplitude waves there is no net measurable mass transport, since there is no net molecular motion, only a net transport of energy and momentum. However, when a sufficiently strong acoustic pressure field is applied into a viscous liquid, non-linear effects set in. In such cases the liquid can start to flow in the same direction as propagation of acoustic waves. This fact is explained as momentum transfer from the wave to the fluid by viscous attenuation of a sound (pressure). Due to spatial variation in pressure amplitude around the acoustic beam and the degree of sound attenuation, shear induced eddies and circulation currents can be generated. The liquid motion or the steady bulk flow within any fluid medium under these influences of acoustic waves is called acoustic streaming [1]. Simply stated, acoustic streaming is a dissipation of the acoustic energy in the form of change of the gradients in the momentum flux [2, 3]. Streaming is only one effect [4] of the propagation of the high intensity acoustic waves. Other effects are cavitation, agitation and oscillatory fluid motion, etc. Acoustic streaming is a second-order steady flow [5], which is superimposed on the dominant acoustic velocity and it is induced by the non-linearities of the acoustic propagation. The absorption of the energy of the sound wave by the fluid is responsible for this induced flow [3, 6]. Acoustic streaming is used widely for non-invasive intervention purposes, both in industry and medicine. Among them, detection of ovarian cysts, detection of blood clotting via ultrasound, convective transport in microfluidic applications, removal of non-specifically bound proteins to allow reuse of biosensors, drug delivery, etc. [7, 8] are popular. One of the trending utilization of acoustic streaming is to generate high efficient

ISSN: 2046-0546 (paper format), ISSN: 2046-0554 (online), http://www.witpress.com/journals
DOI: 10.2495/CMEM-V6-N4-814-826

mixing and heat transfer in different applications [1, 9, 10]. This has become increasingly important when some process conditions and the materials are risky to reach. In literature, the studies that investigated the phenomena of acoustic streaming are limited to qualitative description of the phenomena and very few researchers have looked at acoustic streaming in a quantitative way. Almost all of them have reported about the streaming caused by ultrasound sources. Ref [11], who used a lithotripsy pulse to generate acoustic waves have found almost a linear relationship between the streaming velocity and the generated peak-negative pressures. Ref [6] have developed a CFD model in order to predict the acoustic streaming assuming that the hydrodynamic momentum rate of the incoming jet is equal to the total acoustic momentum rate emitted by the transducer. The laser doppler anemometry (LDA) measurements performed by Ref. [1] validate their CFD model for the visualization of acoustic streaming induced by an ultrasonic horn. References [4, 11] state that the streaming velocity due to any acoustic source within a fluid, is proportional to the intensity and the surface area of the acoustic source (an ultrasound source), the attenuation coefficient of the medium and inversely proportional to the bulk viscosity and the speed of sound in the medium. The numerical study performed by Ref. [12] visualized the cavitation and acoustic streaming as a result of periodic changes in pressure within a liquid medium. The application of low frequency ultrasound is limited to studies that have been done using air as the medium to visualize the streaming patterns and velocity. Studies of acoustic streaming within non-Newtonian liquids are very limited except in medical field with regarding to the biological applications. From the study performed by Ref. [10], they have experienced the acoustic streaming produced by ultrasonic transducers in highly viscous fluid. Ref. [8] have presented the effects of non-Newtonian viscosity and the power law model on non-linear acoustofluidics by claiming that streaming velocity is highly dependent on the viscosity model of the blood and increasing ultrasonic frequency or intensity, amplifies the streaming velocity Ref. [13], who used LDA to study the acoustic and streaming velocity inside a cylindrical standing-wave resonator filled with air mention that the magnitude of the streaming is dependent on fluid viscosity with temperature. However, Ref. [5] have performed a similar type of experiment using LDA, but in isothermal conditions to prove the non-linear phenomena of oscillatory flows and the efficiency degradation of thermoacoustic devices. According to the study performed by Ref. [7] to predict the acoustic streaming phenomenon in Newtonian and non-Newtonian fluids, the streaming velocities predicted for a non-Newtonian fluid are smaller than that in a Newtonian fluid. Visualization of acoustic streaming becomes much more representative by using a non-intrusive technique such as LDA or PIV if turbulent flow is dominating. The intrusive measurement techniques or visual observations techniques like streak photography to estimate the velocity magnitude is not accurate enough [1] in this regard. PIV is based on video images of the illuminated fluid flow plane using seeding particles and produces an instantaneous two dimensional velocity vector field [14]. Ref.[4] have used PIV technique to visualize acoustic streaming and established a positive linear relationship between the ultrasonic intensity and the peak streaming velocity while Ref. [11] suggest that PIV is a good non-intrusive technique to estimate the peak-pressures in streaming applications. References [15, 16] have used synchronized PIV technique to measure the acoustic and streaming velocity fields simultaneously. The experimental values of the mean acoustic velocity and streaming velocities obtained from PIV are in good agreement with the theoretical values confirming the applicability of synchronized PIV technique.

The background for these preliminary acoustic experiments at low frequency (lower part of the acoustic range) is to investigate whether they can make any considerable influence to

the rheology of drilling fluids and subsequently the particle settling within non-Newtonian drilling fluids. It is obvious that, scaling up of such acoustic processes has shown to be difficult due to the interactions between the sound field and the subsequently generated flow. For that, better analytical and numerical studies of this type of low frequency acoustic streaming are important and valuable. However, a comprehensive experimental study is necessary to get a better insight into the streaming velocity fields within Newtonian and non-Newtonian fluids to think and design further experiments confining to the aim. Therefore, this study considers the acoustic streaming in both Newtonian and non-Newtonian liquids at a very low frequency range and describes how the streaming velocity is affected in both qualitative and quantitative manner when the frequency, input power as well as the fluid rheology is changed.

2 MATERIALS AND METHODS

In this work acoustic streaming was studied with acoustic waves generated from a low frequency underwater acoustic transducer in an open liquid container. The experimental setup is shown in Fig. 1. This rectangular channel is made of glass with the dimensions of 0.97 m × 0.13 m × 0.28 m. De-ionized water and 1 g/L PAC were used as the Newtonian and non-Newtonian fluids, respectively. The white/off-white colour regular PAC granular powder (with a bulk density of 400–880 kg/m^3) provided by M–I Swaco, England was used to prepare the polymer solution. A volume of 20 L liquid was used for all the test runs. After performing the test runs with deionized water, 1 g/L PAC solution was introduced gradually to the same liquid channel in small quantities to identify the PAC concentration that does not show any streaming or any induced flow. A low frequency underwater acoustic transducer BII-7531 (D × H = 60 × 40 mm) provided by Benthowave Instrument Inc. Canada, with an output frequency ranging from 600 Hz to 15 kHz was utilized. Sonication was provided as continuous sinusoidal waves in a range of frequencies and amplitudes as mentioned in Table 1. The transducer was positioned at the centre of the liquid body 12 cm away from the left wall of the open channel as shown in Fig. 1. The two inside ends of the rectangular channel were covered using sponge type sound absorbing material to avoid any sound reflection from the end walls. A function generator model 33220A from Agilent

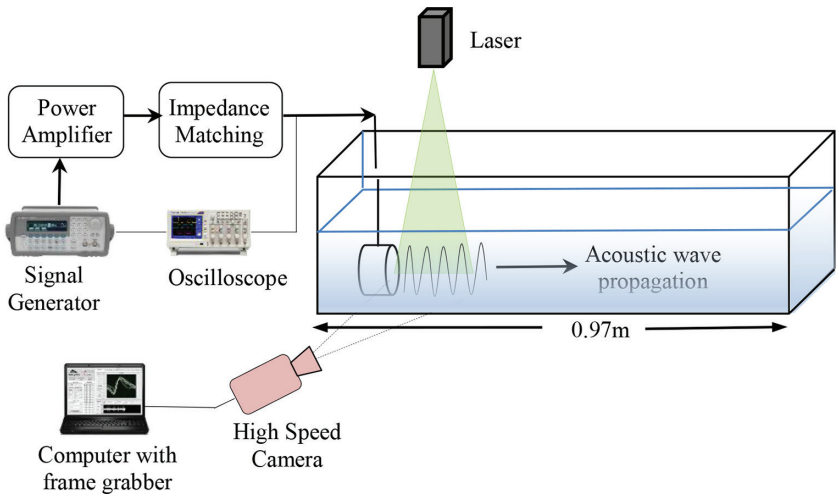

Figure 1: Sketch of the experimental set up.

Table 1: Test matrix used for the experiments.

Frequency (kHz)	Amplitude in terms of supply voltage (mV) from Signal Generator	Input voltage to the acoustic transducer after amplification (V_{RMS})	Input power to the acoustic transducer after amplification (W_{RMS})
Effect of frequency			
4	500	251	11.5
5	500	256	13.4
6	500	263	16.6
Effect of power input			
6	400	213	10.8
6	500	263	16.6
6	600	301	20.3
6	700	328	25.1
6	800	342	27.1

Technologies was used to generate the sinusoidal waves of different frequencies and amplitudes. The accuracy of the generated frequency and amplitude are 1 μHz and 0.1 mV, respectively. A linear power amplifier (BII-5061), which has a maximum power output of 200 W at +48 VDC amplified the signal from the function generator. The amplified signal was fed to an impedance matching unit (BII-6010) in order to match the high acoustic impedance of the transducer. Voltage and the current of the amplified signal just upstream of the transducer was read from an Oscilloscope (Tektronix TDS 2024C), where the input power to the transducer was also computed using the MATH function of it. The effect of input electrical power and frequency of an acoustic wave on the streaming velocity in a Newtonian fluid was studied in axial and radial directions. The effect of the fluid rheology on acoustic streaming was studied by gradually adding some small quantities of 1g/L PAC solution to the deionized water at a constant frequency of 6 kHz and amplitude of 700 mV. All experiments were conducted in room temperature at 21^0C. The rheological measurements were taken from Anton Paar MCR 302 viscometer at constant temperature and pressure.

2.1 The PIV system

The two-dimensional velocity fields inside the channel were measured using PIV technique. A Basler A800-510 μm colour camera (500 fps in full resolution 800 × 600) equipped with a 532 nm green laser (Photon DPGL-2200) was used to capture the images. All the images for the test series were captured at 100 fps with a resolution of 688 × 400 pixels and the measurements were made in a plane parallel to the channel length. The laser plane was illuminated vertically through the centre of the fluid filled tank. Polyamide seeding particles (PSP-50 from DANTEC Dynamics) with a mean diameter of 50 μm were added to the liquids as light scattering tracer ('seeding') particles for measuring the field velocity profile. Data acquisition was continued for sufficiently long time in order to allow the streaming flow to achieve its steady state profiles.

2.2 Image analysis

To calculate the streaming velocity field, acquired images were processed using PIVlab [17], which is a Digital Particle Image Velocimetry (DPIV) tool developed in MATLAB. The tool calculated the particle displacement for groups of particles by evaluating the cross-correlation of many small sub images (interrogation areas). The camera was set so that the image contained the whole region with the transducer and the streaming flow approximately up to 18 cm downstream the transducer. For image processing, a partial section that illustrates the streaming flow within the liquid medium was selected as the region of interest rather than the entire image captured. All the images were pre-processed using contrast limited adaptive histogram equalization (CLAHE) and some background noise was removed using high pass filter. For the PIV settings FFT window deformation was adopted with interrogation area with 3 passes. Gaussian 2 x 3 point was used as the sub-pixel estimator. Regarding post-treatment of correlated frames and for data validation, a vector velocity threshold with a high standard deviation value was set.

3 RESULTS AND DISCUSSION

The results of the experiments are presented in this section. The PIV technique was used for the quantification of streaming velocity and different features of the streaming velocity maps are discussed within this section. The effect of applied frequency, input voltages to the transducer and also rheology of the fluid medium are investigated with different visual models. All the velocity profiles presented in this section are regressed using Gaussian model with an accuracy of $R^2 > 90\%$.

3.1 Transient flow development

The transient flow development in pure deionized water due to the application of acoustic waves from the low frequency underwater transducer is shown in Fig. 2. Results shown here are from the test carried out at a frequency of 6 kHz and an input voltage of 700 mV to the signal generator, which provided an electrical input power of $25.1W_{RMS}$. Figure 2 shows a typical map of an acoustically induced flow with its temporal propagation in front of the transducer face for 8 seconds. The flow originates from the transducer as a result of sonication. The streaming is highest along the beam centreline. A maximum flow velocity was reached at a certain distance from the transducer, and beyond this distance the streaming was gradually diffused. This velocity 'smearing' is attributed to the attenuation effects within the liquid medium. Strong streaming was formed in the direction of the beam-axis immediately after the transducer was switched on (at t = 0 s) and the spatial distribution of the velocity vectors is complex with several local peaks and vortices. The temporal movement of the acoustic wave front is similar to a streaming jet confirming the establishment of Ref. [2], where the acoustic streaming takes the form of an inertially dominated turbulent jet at powers above 4×10^{-4} W. The jet-like flow movement sets up large-scale circulations within the liquid body and eventually interact back and modify the streaming jet. The shape of the visual model of the induced flow is much distorted and vigorous as it propagates and that drives away the particles from the transducer along the channel.

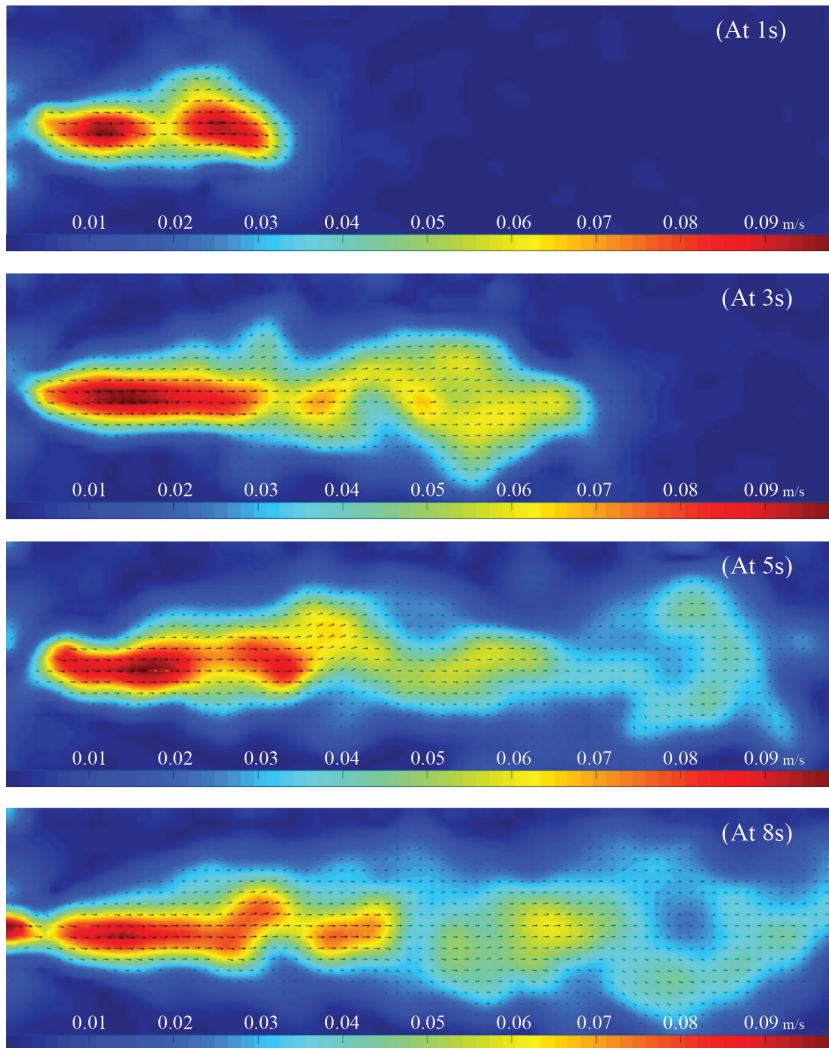

Figure 2: Transient flow development in deionized water for 8s.

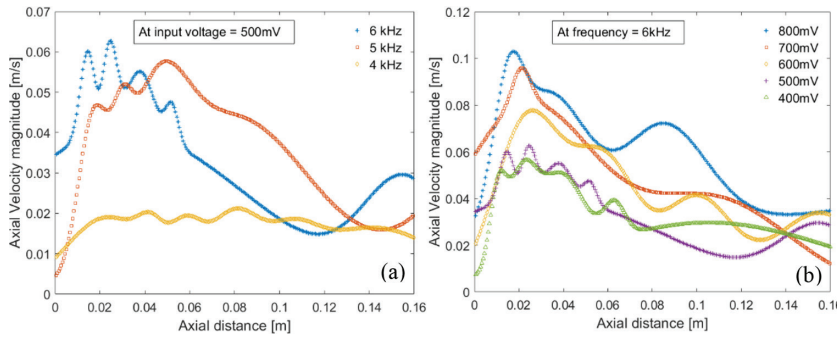

Figure 3: Axial velocity distribution in pure water at 30s. (a) At constant input voltage; (b) At constant frequency. (*Voltage mentioned here is the input from the signal generator)

3.2 Velocity magnitude in axial direction at steady state

Figure 3 shows how the streaming velocity varies within pure water along a horizontal axis which contains the peak streaming velocity. The acoustic transducer is placed at the left side and the results shown here are taken when the flow is assumed to have achieved its steady state at 30 s. Figure 3(a) shows the variation of axial streaming velocity for different frequencies when the input power to the transducer is kept constant at 500 mV and Fig. 3(b) shows the variation of axial streaming velocity when the input power to the transducer varies at a frequency of 6 kHz. As shown in the transient flow development in Fig. 2, the streaming velocity is dying out in the fluid medium when it is moving away from the transducer. It is observed that the peak velocity is obtained only one time along the beam axis closer to the acoustic source and some other minor peaks that are not so strong can also present. Therefore, it can be said that the acoustic streaming is significant in the proximity of the transducer and decreases as the flow moves away from the transducer. This is due do the attenuation of the acoustic wave and this attenuation increases with the distance from the transducer. The shape of the curves is far from being sinusoidal and is actually much distorted. There can be seen a strong asymmetry of the axial velocity, which drives away the particles from the transducer which can be explained due to the non-linear phenomenon and probably the presence of superior harmonics, distorting the sinus. This asymmetric pattern of axial streaming velocity distribution is same for all the frequencies and input power values investigated. Even so, according to Fig. 3(a), it can be seen that the peak streaming velocity increases when the applied frequency of the transducer is increased. That is same for the axial velocity curves shown in Fig. 3(b), where the peak streaming velocity increases when the input electrical power to the acoustic source is increased. The maximum peak axial velocity detected was 9.94 cm/s at a frequency of 6 kHz and at an input voltage of 800 mV to the signal generator, which resulted in a input electrical power of 27.1W_{RMS}.

3.3 Velocity magnitude in radial direction at steady state

Figure 4 shows how the radial streaming velocity varies within pure water along a line normal to the beam axis where the peak velocity appeared. The results shown here are taken when the flow is assumed to have achieved its steady state at 30s. The velocity profile in radial

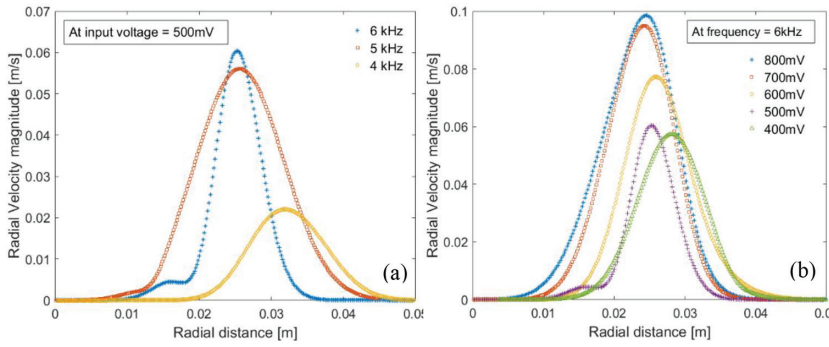

Figure 4: Radial velocity distribution in pure water at 30s. (a) At constant input voltage; (b) At constant frequency. (*Voltage mentioned here is the input from the signal generator)

direction, perpendicular to the beam-axis, is relatively symmetrical and has its maximum at the centre. According to Fig. 4(a), it can be seen that the radial velocity of the acoustically induced flow within the water channel increases as the applied frequency of the acoustic source is increased. The bell-shape of the three curves in Figure 4(a) illustrates the effect of frequency on the velocity distribution in such a way that higher frequencies provide more intensified push up at the centreline of the beam. When the frequency is lowered, the velocity tends to distribute to either sides of the beam axis since they are not having much intensified effect as it was at higher frequencies. Variation of the radial streaming velocity with the input electrical power to the transducer is shown in Fig. 4(b) and, this clearly shows how the tip of the bell-shaped velocity profile moves towards the right direction. This also confirms the axial velocity distributions presented in Fig. 3 in a way that when the intensity of the input signal is reduced, the forcing effect of the bulk liquid flow is also reduced. As a result of this, the peak velocity may not occur exactly at the centre line or the beam axis, but at places little lower than the beam axis.

3.4 Peak velocity variation

Variation of the peak streaming velocity (V_p) with input frequency and power is shown in Fig. 5. This is the same peak velocity displayed in Fig. 3 after the flow is assumed to have obtained its steady state and the two velocity components; u-velocity (axial component) and v-velocity (radial component) are also incorporated to describe the dominant direction of the flow. The peak streaming velocity (V_p) is composed of the two velocity components u and v as described in eqn (1).

$$V_p = \sqrt{u^2 + v^2} \tag{1}$$

It is seen that V_p increases with input frequency and also with the input power to the transducer as it was already discussed in the previous section and already stated by Refs. [4, 18]. The most important fact here is, the radial component of the velocity (v-velocity) is far less than the axial component (u-velocity). This depicts a very firm idea and confirms the visual observations that the flow is mainly driven towards the horizontal direction due to the momentum transfer from the acoustic wave. According to Fig. 5(a), the v-velocity component has been increased with the frequency which can be described as the flow is developing towards

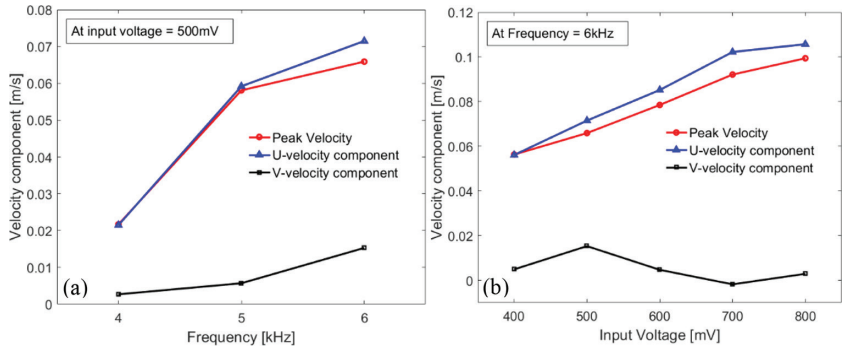

Figure 5: Variation of peak streaming velocity in pure water at 30s. (a) At constant input voltage; (b) At constant frequency. (*Voltage mentioned here is the input from the signal generator)

more vortex type patterns. However, according to Fig. 5(b), the v-velocity component is not much responsive to the input power of the acoustic source. This assures that the flow is more or less intensified with the power input and focusing towards the bulk axial movement away from the transducer. It is important to mention that, the irradiated acoustical energy can differ from absorbed energy in several times and this difference depends on many factors. Here also, in this study, authors are talking about the input electrical power to the acoustic transducer and not the power of sonication process within the liquid medium. To determine the efficiency of acoustic field, it is necessary to know acoustical energy introduced and absorbed in the liquid volume.

3.5 Velocity vectors and streamlines

The length of the vector components (shown in Fig. 6) quantifies the acoustic streaming velocity in pure water for the frequency of 6 kHz and input voltage of 700 mV to the signal generator. Here also, the results are taken when the flow is assumed to have achieved its steady state at 30 s. Figure 6 shows only one particular case of the experiments and vector plots for other cases are not presented here for brevity. When analysing these vector plots, it is observed in all of the cases that maximum flow velocity is observed in the region closer to the acoustic source. At low frequency and low input power, most of the velocity changes occur near the transducer without much distortions on the other side of the liquid channel. That means, the main mixing is observed in the regions near the transducer. However, for the higher frequencies, almost, all of the fluid achieved high velocity and the violent mixing was

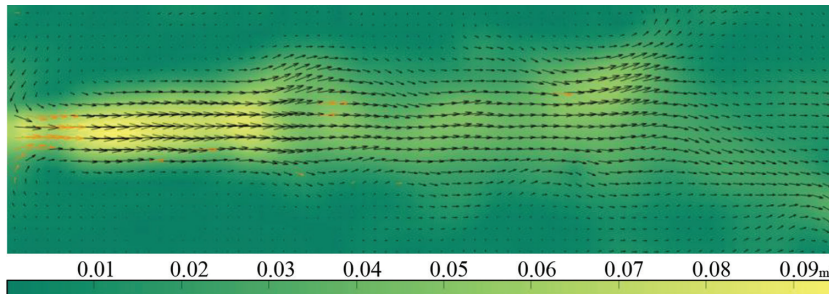

Figure 6: Velocity vector plot in pure water for 6 kHz & 700 mV (steady state at 30s)

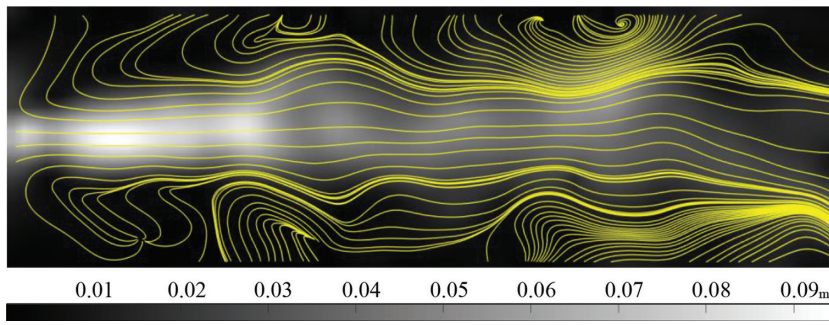

Figure 7: Streamline pattern in pure water for 6 kHz & 700 mV (steady state at 30s).

generated within the channel up to some considerable distance. Velocity vectors give a great insight about the mixing phenomena within the liquid.

Figure 7 shows the stream line pattern for the same case explained above in Fig. 6. The spatial distribution of the velocity vector field is confirmed by the stream line plot which illustrates the complexity of the motion of fluid with several local peaks and vortices. According to Fig. 7, it can be seen that for higher power inputs, the flow reversal takes place near the transducer and flow is in the inward direction. It indicates that there is an entrainment of liquid towards the centre of the transducer due to the high velocity near the source and high-pressure gradient. This phenomenon is evident from the vector plot of the velocity magnitude shown in Fig. 6 also. Some distinct vortices are visible in either sides of the beam axis forming the motion more complex and confirming the statement of [16] which says when the amplitude of the acoustic source increases, circulatory streaming develops and is then distorted to a complicated and irregular structure.

3.6 Effect of fluid rheology on acoustic streaming.

As described in the methodology, polyanionic cellulose (PAC) was used to investigate how the fluid rheology influences the acoustic streaming. That is one of the main objectives of this preliminary study to use acoustic streaming effect on non-Newtonian liquids where particle settling needs to be altered. Known quantities of 1g/L PAC were added gradually in small portions. The streaming flow was the checked for each case as done for the pure water. Figure 8(a) shows the influence of PAC concentration on axial streaming velocity only for some selected cases for brevity. Results shown here are from the test carried out at a frequency of 6 kHz and an input voltage of 700 mV to the signal generator which provided an electrical input power of 25.1 W_{RMS}. And also, the results are taken when the flow is assumed to have achieved its steady state at 30 s.

It can be seen from Fig. 8(a) that the axial streaming velocity is reduced with the added PAC concentration. When the overall PAC concentration within the liquid channel reached 0.19 g/L, the streaming flow was completely disappeared. Similar to the axial streaming velocity profiles seen for pure water in Fig. 3, here also the streaming velocity is dying out in the non-Newtonian fluid medium further away from the transducer. However, it is important to notice that the flow induced by the acoustic waves within the non-Newtonian medium is smearing out quickly at a lower axial distance than that we observed for pure water. This

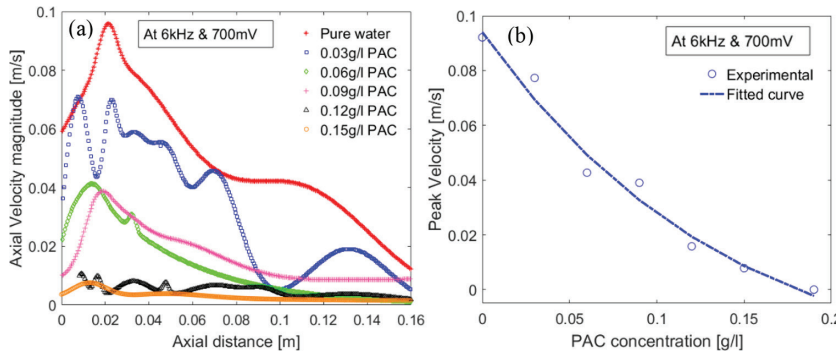

Figure 8: (a) Axial velocity distribution in PAC; (b) Peak velocity variation with PAC concentration. (*Voltage mentioned here is the input from the signal generator)

phenomena is attributed to the strong attenuation property of non-Newtonian liquid. It is observed that the peak velocity is obtained only one time along the beam axis closer to the acoustic source before it smears out. Figure 8(b) illustrates how the peak velocity magnitude is reducing with the added PAC concentration. The peak velocity started with a value of 9.21 cm/s for pure water until it reaches zero when the PAC concentration became 0.19 g/L. The experimental peak velocity magnitudes at different concentrations were well fitted by an exponential curve shown in eqn (2) with an accuracy of $R^2 = 97.76\%$.

$$V_p = a * \exp\left(b * C_{PAC}\right) + c * \exp\left(d * C_{PAC}\right) \tag{2}$$

Where, C_{PAC} is the concentration of PAC in g/L and a, b, c and d are constants with the values of 6.992, -4.107, -6.898 and -4.032 respectively. The rheological properties of the resulted PAC solution with the concentration of 0.19 g/L were measured after the experiments and the parameters of that solution according to the power law are n = 0.97 and $K=3.3 \times 10^{-3}$ $Pa.s^n$, where n is the behaviour index and K is the consistency index of the fluid.

4 CONCLUSION

The set of experiments were conducted to visualize the acoustic streaming produced by a low frequency underwater acoustic transducer in both Newtonian and non-Newtonian fluids. PIV technique was used for quantification of the streaming velocity. The features of the streaming velocity maps, vector plot and streamline pattern were presented for some selected cases. It was observed that, the streaming is highest along the beam centreline and the maximum peak velocity along the transducer beam is in the axial position. Acoustic streaming is significant in the proximity of the transducer and decreases as the flow moves away from the transducer due to the attenuation of the acoustic wave and this attenuation increases with the distance from the transducer. The temporal movement of the acoustic wave front is similar to a streaming jet. Streaming depends on the applied frequency and the input voltage (power). Streaming velocity vectors give a great insight about the mixing phenomena within the liquid and the vortices visible in streamline plots confirm the complexity and the non-linearity of the fluid flow induced by the acoustic pressure field. The peak streaming velocity (V_p) measured was in the range of 2.1–9.9cm/s for pure water and that depends on the supply frequency and the input voltage settings to the transducer. The streaming velocities observed for non-Newtonian fluid is smaller than that for the Newtonian fluid confirming the fact that the wave attenuation is much higher in non-Newtonian fluids.

ACKNOWLEDGEMENTS

The authors would like to acknowledge the valuable support provided by H.A. Rabenjafimanantsoa, Milad Khatibi from Department of Petroleum Engineering & Jon fidjeland, Romuald K. Bernacki from department of computer and electrical engineering in university of stavanger. Authors gratefully acknowledge the Norwegian Research Council for funding this study under the project “NFR Improved Model Support in Drilling Automation”.

REFERENCES

[1] Kumar, A., Kumaresan, T., Pandit, A.B. & Joshi, J.B., Characterization of flow phenomena induced by ultrasonic horn. *Chemical Engineering Science,* **61**(22), pp. 7410–7420, 2006.
https://doi.org/10.1016/j.ces.2006.08.038

[2] Lighthill, S.J., Acoustic streaming. *Journal of Sound and Vibration,* **61**(3), pp. 391–418, 1978.
https://doi.org/10.1016/0022-460x(78)90388-7
[3] Nyborg, W.L., Acoustic streaming due to attenuated plane waves. *The Journal of the Acoustical Society of America,* **25**(1), pp. 68–75, 1953.
https://doi.org/10.1121/1.1907010
[4] Frenkel, V., Gurka, R., Liberzon, A., Shavit, U. & Kimmel, E., Preliminary investigations of ultrasound induced acoustic streaming using particle image velocimetry. *Ultrasonics,* **39**(3), pp. 153–156, 2001.
https://doi.org/10.1016/s0041-624x(00)00064-0
[5] Ellier, E.S., Bailly, Y., Girardot, L., Ramel, D. & Nika, P., *Acoustic streaming measurements by PIV*, presented at the 15th International Symposium on Flow Visualization, Minsk, Belarus, June 25–28, 2012.
[6] Trujillo, F.J. & ,Knoerzer, K., *CFD modelling of the acoustic streaming induced by an ultrasonic horn reactor*, Seventh international conference on CFD in the minerals and process industries, CSIRO, Melbourne, Australia, 2009.
[7] Sankaranarayanan, S.K., Singh, R. & Bhethanabotla, V.R., Influence of non-newtonian fluid dynamics on SAW induced acoustic streaming in view of biological applications, in *Sensors, 2011 IEEE*, pp. 1546–1549, 2011.
[8] Aayani, R., Shahidian, A. & Ghassemi, M., Numerical investigation of non-newtonian blood effect on acoustic streaming. *Journal of Applied Fluid Mechanics,* **9**, pp. 173–176, 2016.
[9] Groznova, A., *Modelling of ultrasound assisted mixing in Newtonian and non-Newtonian liquids*, 2014.
[10] Rabenjafimanantsoa, H.A., Wrobel, B.M. & Time R.W., PIV Visualization of acoustic streaming in Non-Newtonian fluid. *Annuals Transactions of the Nordic Rheology Society,* **17**, 2009.
[11] Choi, M., Doh, D.H., Cho, C.H., Kang, K.S., Paeng, D.G., Ko, N.H., Kim, K.S., Rim, G.H. & Coleman, A.J., Visualization of acoustic streaming produced by lithotripsy field using a PIV method. *Journal of Physics: Conference Series*, **1**(1), pp. 217–223, 2004.
https://doi.org/10.1088/1742-6596/1/1/048
[12] Abolhasani, M., Rahimi, M., Dehbani, M. & Shabanian, S.R., *CFD modeling of low, medium and high frequency ultrasound waves propagation inside a liquid medium*. Presented at the 4rd National Conference on CFD Applications in Chemical & Petroleum Industries, Ahwaz, Iran, 2012.
[13] Thompson, M.W. & Atchley, A.A., Simultaneous measurement of acoustic and streaming velocities in a standing wave using laser Doppler anemometry. *The Journal of the Acoustical Society of America,* **117**(4), pp. 1828–1838, 2005.
https://doi.org/10.1121/1.1861233
[14] Adrian, R.J., Particle-imaging techniques for experimental fluid mechanics. *Annual Review of Fluid Mechanics,* **23**(1), pp. 261–304, 1991.
https://doi.org/10.1146/annurev.fluid.23.1.261
[15] Nabavi, M., Siddiqui, M.H.K. & Dargahi, J., Simultaneous measurement of acoustic and streaming velocities using synchronized PIV technique. *Measurement Science and Technology,* **18**(7), pp. 1811–1817, 2007.
https://doi.org/10.1088/0957-0233/18/7/003

[16] Nabavi, M., Siddiqui, M.H.K. & Dargahi, J., Experimental investigation of the formation of acoustic streaming in a rectangular enclosure using a synchronized PIV technique. *Measurement Science and Technology,* **19**(6), p. 065405, 2008. https://doi.org/10.1088/0957-0233/19/6/065405

[17] Thielicke, W. & Stamhuis, E., PIVlab–Time-Resolved Digital Particle Image Velocimetry Tool for MATLAB, version: 1.32. *Journal of Open Research Software,* **10**, p. m9, 2014.

[18] Chouvellon, M., Largillier, A., Fournel, T., Boldo, P. & Gonthier, Y., Velocity study in an ultrasonic reactor. *Ultrasonics Sonochemistry,* **7**(4), pp. 207–211, 2000. https://doi.org/10.1016/s1350-4177(00)00060-2